COVID-19 vaccine BNT162b1 elicits human antibody and T_H1 T cell responses

https://doi.org/10.1038/s41586-020-2814-7

Received: 16 July 2020

Accepted: 22 September 2020

Published online: 30 September 2020

Check for updates

Ugur Sahin[1,2]✉, Alexander Muik[1], Evelyna Derhovanessian[1], Isabel Vogler[1], Lena M. Kranz[1], Mathias Vormehr[1], Alina Baum[3], Kristen Pascal[3], Jasmin Quandt[1], Daniel Maurus[1], Sebastian Brachtendorf[1], Verena Lörks[1], Julian Sikorski[1], Rolf Hilker[1], Dirk Becker[1], Ann-Kathrin Eller[1], Jan Grützner[1], Carsten Boesler[1], Corinna Rosenbaum[1], Marie-Cristine Kühnle[1], Ulrich Luxemburger[1], Alexandra Kemmer-Brück[1], David Langer[1], Martin Bexon[4], Stefanie Bolte[1], Katalin Karikó[1], Tania Palanche[1], Boris Fischer[1], Armin Schultz[5], Pei-Yong Shi[6], Camila Fontes-Garfias[6], John L. Perez[7], Kena A. Swanson[7], Jakob Loschko[7], Ingrid L. Scully[7], Mark Cutler[7], Warren Kalina[7], Christos A. Kyratsous[3], David Cooper[7], Philip R. Dormitzer[7], Kathrin U. Jansen[7] & Özlem Türeci[1]

An effective vaccine is needed to halt the spread of the severe acute respiratory syndrome coronavirus-2 (SARS-CoV-2) pandemic. Recently, we reported safety, tolerability and antibody response data from an ongoing placebo-controlled, observer-blinded phase I/II coronavirus disease 2019 (COVID-19) vaccine trial with BNT162b1, a lipid nanoparticle-formulated nucleoside-modified mRNA that encodes the receptor binding domain (RBD) of the SARS-CoV-2 spike protein[1]. Here we present antibody and T cell responses after vaccination with BNT162b1 from a second, non-randomized open-label phase I/II trial in healthy adults, 18–55 years of age. Two doses of 1–50 µg of BNT162b1 elicited robust $CD4^+$ and $CD8^+$ T cell responses and strong antibody responses, with RBD-binding IgG concentrations clearly above those seen in serum from a cohort of individuals who had recovered from COVID-19. Geometric mean titres of SARS-CoV-2 serum-neutralizing antibodies on day 43 were 0.7-fold (1-µg dose) to 3.5-fold (50-µg dose) those of the recovered individuals. Immune sera broadly neutralized pseudoviruses with diverse SARS-CoV-2 spike variants. Most participants had T helper type 1 (T_H1)-skewed T cell immune responses with RBD-specific $CD8^+$ and $CD4^+$ T cell expansion. Interferon-γ was produced by a large fraction of RBD-specific $CD8^+$ and $CD4^+$ T cells. The robust RBD-specific antibody, T cell and favourable cytokine responses induced by the BNT162b1 mRNA vaccine suggest that it has the potential to protect against COVID-19 through multiple beneficial mechanisms.

Severe acute respiratory syndrome coronavirus 2 (SARS-CoV-2), which was identified in China in December 2019, causes coronavirus disease 2019 (COVID-19)—a severe, acute respiratory syndrome with a complex, highly variable disease pathology. On 11 March 2020, the World Health Organization (WHO) declared the SARS-CoV-2 outbreak a pandemic. As of 16 September 2020, more than 29 million cases have been reported worldwide, with over 930,000 deaths[2]. The severe and worldwide effect of the pandemic on human society calls for the rapid development of safe and effective therapeutics and vaccines[3].

Lipid nanoparticle (LNP)-formulated mRNA vaccine technology allows the delivery of precise genetic information together with an adjuvant effect to antigen-presenting cells[4]. The prophylactic effectiveness of this technology against multiple viral targets has been proven in preclinical models[5–7]. LNP- and liposome-formulated RNA vaccines for preventing infectious diseases or treating cancer have been shown in clinical trials to be safe and well-tolerated[8]. mRNA is transiently expressed and does not integrate into the genome. It is molecularly well defined, free from materials of animal origin, and synthesized by an efficient, cell-free in vitro transcription process from DNA templates[5,9,10]. The fast and highly scalable mRNA manufacturing and LNP formulation processes enable rapid production of manyvaccine doses[6,7,11], making it suitable for rapid vaccine development and pandemic vaccine supply.

Two phase I/II umbrella trials in Germany and the USA are investigating several LNP-encapsulated RNA vaccine candidates developed in 'Project Lightspeed', the joint BioNTech-Pfizer COVID-19 RNA vaccine development program. Recently, we reported interim data obtained in the USA trial (NCT04368728) for the most advanced candidate, BNT162b1[1]. BNT162b1 encodes the receptor-binding domain (RBD) of the SARS-CoV-2 spike protein, a key target of neutralizing antibodies. The RBD antigen expressed by BNT162b1 is fused to a T4 fibritin-derived 'foldon' trimerization domain to increase its immunogenicity by

[1]BioNTech, Mainz, Germany. [2]TRON gGmbH–Translational Oncology at the University Medical Center of the Johannes Gutenberg, Mainz, Germany. [3]Regeneron Pharmaceuticals, Tarrytown, NY, USA. [4]Bexon Clinical Consulting, Upper Montclair, NJ, USA. [5]CRS Clinical Research Services Mannheim GmbH, Mannheim, Germany. [6]University of Texas Medical Branch, Galveston, TX, USA. [7]Pfizer, Pearl River, NY, USA. ✉e-mail: ugur.sahin@biontech.de

multivalent display[12]. The RNA is optimized for high stability and translation efficiency[13,14] and incorporates 1-methylpseudouridine instead of uridine to dampen innate immune sensing and to increase mRNA translation in vivo[15]. In the placebo-controlled, observer-blinded USA trial, dosages of 10 µg, 30 µg (prime and boost doses 21 days apart for both dose levels) and 100 µg (prime only) were administered. No serious adverse events were reported. Local injection site reactions and systemic events (mostly influenza-like symptoms) were dose-dependent, generally mild to moderate, and transient. RBD-binding immunoglobulin G (IgG) concentrations and SARS-CoV-2 neutralising titres in sera increased with dose level and after the second dose. Fourteen days after the boost dose, geometric mean neutralising titres reached 1.9- to 4.6-fold those seen in a panel of COVID-19 human convalescent sera (HCS).

This study now complements and expands our previous report with available data from the German trial (NCT04380701, EudraCT: 2020-001038-36), providing a detailed characterization of antibody and T cell immune responses elicited by vaccination with BNT162b1.

Study design and analysis set

Between 23 April 2020 and 22 May 2020, 60 participants were vaccinated with BNT162b1 in Germany. Twelve participants for each of the dose level groups (1 µg, 10 µg, 30 µg, and 50 µg) received the first dose on day 1 and a booster dose on day 22 (except for one individual in each of the 10- and 50-µg dose-level cohorts who discontinued participation for reasons not related to the study drug), and 12 participants received a 60-µg prime dose on day 1 only (Extended Data Fig. 1). The study population consisted of healthy males and non-pregnant females with a mean age of 37 years (range 20–56 years) with equal gender distribution. Most participants were white (96.7%) with one African American and one Asian participant (1.7% each; Extended Data Table 1). Preliminary data analysis focused on immunogenicity (Extended Data Table 2).

Preliminary safety and tolerability data

In brief, there were no serious adverse events and no withdrawals due to related adverse events for any dose. Similar to the USA trial, most of the reported solicited systemic events in the 10-µg and 30-µg groups were due to reactogenicity, with a typical onset within the first 24 h of immunization (Extended Data Fig. 2). Injection site reactions within 7 days of the prime or boost doses mainly involved pain and tenderness. Reactogenicity was dose-dependent, and was more pronounced after the boost dose. The associated symptomatology, such as fever, chills, headache, muscle pain, joint pain, injection site pain, and tenderness, was mostly mild or moderate, with occasional severe (grade 3) manifestations. In the 30-µg dose level cohort, 2 out of 12 (16.7%) subjects experienced severe local reactogenicity; 6 out of 12 (50%) subjects reported severe systemic reactogenicity (primarily headache, chills, fatigue or muscle pain); and 1 subject out of 12 (8.3%) reported fever. These adverse events were transient, resolved spontaneously or were manageable with simple measures (for example, paracetamol). Because of the reactogenicity reported after the 50-µg boost dose, participants who had received an initial 60-µg dose did not receive a boost injection.

Although there were no relevant changes in routine clinical laboratory values after vaccination with BNT162b1, vaccinated participants showed a transient increase in C-reactive protein (CRP) and a temporary reduction in blood lymphocyte counts, both of which were dose-dependent (Extended Data Fig. 3). CRP is an inflammatory serum protein that has previously been described as biomarker for various infectious disease vaccines and an indicator of vaccine adjuvant activity[16–19]. Our previous clinical experience with RNA vaccines suggests that the transient decrease in lymphocytes is likely to be attributable to innate immune stimulation-related redistribution of lymphocytes into lymphoid tissues[20]. Concomitant neutropenia was not observed.

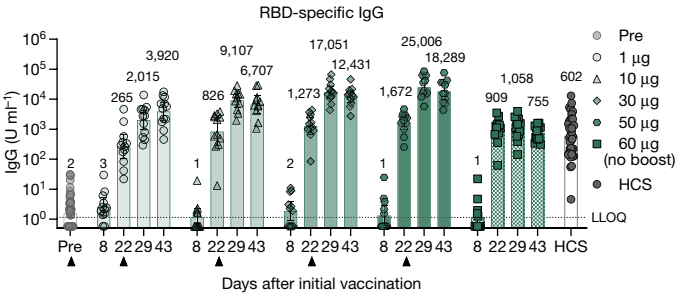

Fig. 1 | BNT162b1-induced IgG concentrations. Vaccination schedule and serum sampling are described in Extended Data Fig. 1. Participants were immunized with BNT162b1 on days 1 (all dose levels) and 22 (all dose levels except 60 µg) ($n = 12$ per group; from day 22 $n = 11$ for the 10 µg and 50 µg cohorts). Pre-dose responses across all dose levels were combined. COVID-19 convalescent samples (HCS, $n = 38$) were obtained at least 14 days after PCR-confirmed diagnosis and at a time when the donors were no longer symptomatic. Each serum was tested in duplicate and GMC plotted. For values below the lower limit of quantification (LLOQ) = 1.15, LLOQ/2 values were plotted. Arrowheads indicate days of vaccination. Checked bars indicate that no boost vaccination was performed. Data shown as group GMC (values above bars) with 95% confidence interval (CI).

Both CRP levels and lymphocyte counts are considered pharmacodynamics markers for the mode-of-action of RNA vaccines.

Vaccine-induced antibody responses

Concentrations of RBD-binding IgG and SARS-CoV-2-neutralizing titres were assessed at baseline, 7 and 21 days after the BNT162b1 priming dose (days 8 and 22), and 7 and 21 days after the boost dose (days 29 and 43), except for the 60-µg cohort, which received a priming dose only (Fig. 1, Extended Data Table 3).

Immunized participants showed a strong, dose-dependent vaccine-induced antibody response. Twenty-one days after the priming dose (for the four dose levels ranging from 1 to 50 µg), geometric mean concentrations (GMCs) of RBD-binding IgG had increased in a dose-dependent manner, with GMCs ranging from 265 to 1,672 units (U) ml^{-1} (Fig. 1). Seven days after the boosting dose (day 29), RBD-binding IgG GMCs in participants vaccinated with 1–50 µg BNT162b1 showed a strong, dose-dependent booster response ranging from 2,015 to 25,006 U ml^{-1}. On day 43 (21 days after boost), RBD-binding antibody GMCs were in the range of 3,920–18,289 U ml^{-1} in BNT162b1-vaccinated individuals, as compared to a GMC of 602 U ml^{-1} measured in a panel of convalescent sera from 38 patients who had been infected with SARS-CoV-2. The patients were 18–83 years of age, and sera were drawn at least 14 days after diagnosis confirmed by polymerase chain reaction (PCR). In the 60 µg dose-level cohort, which received a priming dose only, the RBD-binding IgG GMC was 755 U ml^{-1} by day 43, indicating that a boosting dose is necessary to increase antibody concentrations.

Geometric mean titres (GMTs) of SARS-CoV-2 neutralizing antibodies increased modestly in a dose-dependent manner 21 days after the priming dose (Fig. 2a, Extended Data Table 4). Substantially higher serum-neutralising GMTs were achieved 7 days after the booster dose, reaching 36 (1 µg dose level), 158 (10 µg dose level), 308 (30 µg dose level), and 578 (50 µg dose level), compared to 94 for the convalescent serum panel. On day 43 (21 days after the boost), the neutralizing GMTs and RBD-binding GMCs decreased (with the exception of the 1 µg dose group). Serum virus-neutralizing GMTs were strongly correlated with RBD-binding IgG GMCs (Fig. 2b), and the vaccine elicited lower ratios of serum-neutralizing GMT to RBD-binding IgG GMC than did infection with SARS-CoV-2. In summary, the antibody responses elicited by BNT162b1 in study BNT162-01 largely mirrored those observed in the USA study[1].

To demonstrate the breadth of the neutralizing response, we tested sera from vaccinated participants against a panel of 16 SARS-CoV-2 RBD

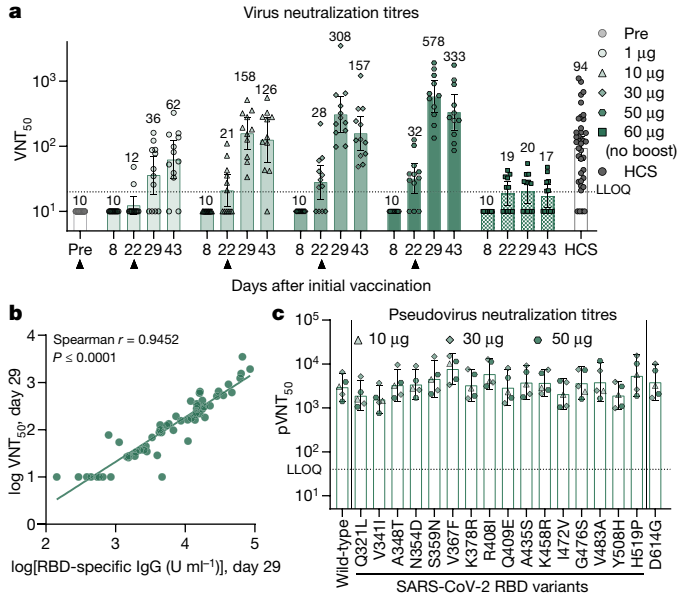

Fig. 2 | BNT162b1-induced virus neutralization titres. Vaccination schedule and serum sampling are described in Extended Data Fig. 1 and participants were immunized as in Fig. 1. **a**, SARS-CoV-2 50% neutralization titres (VNT_{50}) in immunized participants and patients who had recovered from COVID-19 (HCS). Each serum was tested in duplicate and GMT plotted. For values below the LLOQ = 20, LLOQ/2 values were plotted. Arrowheads indicate days of vaccinations. Checked bars indicate that no boost vaccination was performed. Data shown as group GMTs (values above bars) with 95% CI. **b**, Nonparametric Spearman correlation of recombinant RBD-binding IgG GMCs (as in Fig. 1) with VNT_{50} from sera collected on day 29. **c**, Pseudovirus 50% neutralization titres ($pVNT_{50}$) across a pseudovirus panel with 17 SARS-CoV-2 spike protein variants including 16 RBD mutants and the dominant spike protein variant D614G (dose level 10 μg, $n = 1$; dose levels 30 and 50 μg, $n = 2$ representative day 29 sera). Each serum was tested in duplicate and GMT plotted. LLOQ = 40. Data shown as group GMT with 95% CI.

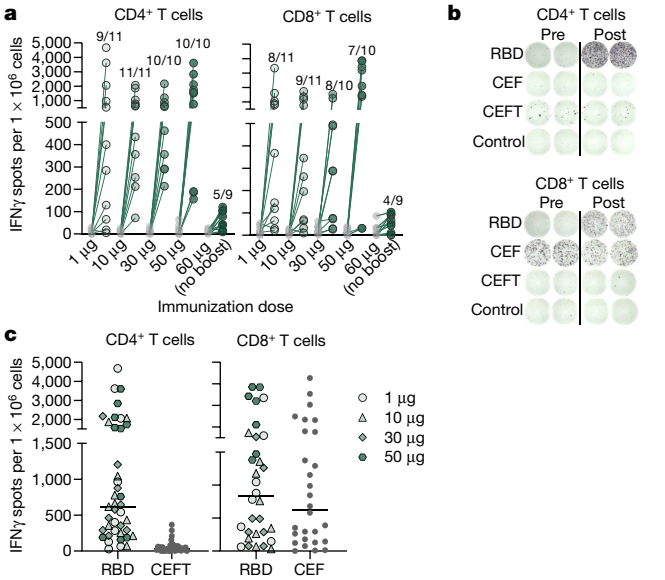

Fig. 3 | Frequency and magnitude of BNT162b1-induced CD4⁺ and CD8⁺ T cell responses. The vaccination schedule is described in Extended Data Fig. 1. PBMCs obtained on day 1 (pre-prime) and on day 29 (7 days after boost for cohorts 1 and 10 μg, $n = 11$ each; 30 and 50 μg, $n = 10$ each; 28 days after prime for the 60 μg cohort, $n = 9$) were enriched for $CD4^+$ or $CD8^+$ T cell effectors and separately stimulated overnight with an overlapping peptide pool representing the vaccine-encoded RBD for assessment in direct ex vivo IFNγ ELISpot. Common pathogen T cell epitope pools CEF (CMV, EBV, influenza virus HLA class I epitopes) and CEFT (CMV, EBV, influenza virus, tetanus toxoid HLA class II epitopes) served to assess general T cell reactivity and cell culture medium served as negative control. Each data point represents the normalized mean spot count from duplicate wells for one study participant, after subtraction of the medium-only control (**a**, **c**). **a**, RBD-specific $CD4^+$ and $CD8^+$ T cell responses for each dose cohort. Ratios above post-vaccination data points are the number of participants with a detectable $CD4^+$ or $CD8^+$ T cell response out of the total number of tested participants per dose cohort. **b**, Exemplary $CD4^+$ and $CD8^+$ ELISpot images for a 10-μg cohort participant. **c**, RBD-specific $CD4^+$ and $CD8^+$ T cell-responses in all participants who received prime and boost vaccination ($n = 42$) with a positive response to RBD and their baseline CEFT- and CEF-specific T cell responses. Horizontal bars indicate median.

variants identified through publicly available information[21] and the dominant (non-RBD) spike variant D614G[22] in pseudovirion neutralization assays. Sera collected 7 days after the second dose of BNT162b1 showed high neutralizing titres to each of the SARS-CoV-2 spike variants (Fig. 2c, Extended Data Table 5).

Vaccine-induced T cell responses

$CD4^+$ and $CD8^+$ T cell responses in individuals immunized with BNT162b1 were characterized before the priming vaccination (day 1) and on day 29 (7 days after the boost vaccination for the 1–50 μg cohorts) using direct ex vivo IFNγ enzyme-linked immunosorbent spot (ELISpot) assay with peripheral blood mononuclear cells (PBMCs) from 51 participants across the 1 μg to 60 μg dose-level cohorts (Fig. 3). In this assay, $CD4^+$ or $CD8^+$ T cell effectors were stimulated overnight with overlapping peptides representing the full-length sequence of the vaccine-encoded RBD.

Of 42 participants who had received prime–boost vaccination (the 1 μg to 50 μg cohorts), 40 (95.2%, including all participants treated with 10 μg BNT162b1 or more) mounted RBD-specific $CD4^+$ T cell responses. Although the magnitude of the response varied between individuals, participants with the strongest $CD4^+$ T cell responses to RBD had more than tenfold the memory responses observed in the same participants when stimulated with cytomegalovirus (CMV), Epstein Barr virus (EBV), influenza virus and tetanus toxoid-derived immuno-dominant peptide panels (Fig. 3a–c). In the 60 μg cohort, who had been treated with the priming dose only, both immunogenicity rate (5/9; 55.6%) and response strength were lower than for the other cohorts, indicating the importance of booster vaccination. No $CD4^+$ T cell responses were detectable at baseline, except for one participant in the 50 μg dose cohort with a low number of pre-existing RBD-reactive $CD4^+$ T cells, which increased substantially after vaccination (normalized mean spot count from 63 to 1,519). For two participants from the 1 μg cohort the baseline data could not be evaluated. The strength of RBD-specific $CD4^+$ T cell responses correlated positively with both RBD-binding IgG and SARS-CoV-2-neutralizing antibody titres (Extended Data Fig. 4a, b), consistent with the concept of intramolecular help[23]. The two participants immunized with 1 μg BNT162b1 who lacked a $CD4^+$ response had no detectable virus-neutralizing titres (VNT_{50}) (Extended Data Fig. 4b).

Among participants who showed any vaccine-induced $CD8^+$ T cell response (32/42 participants receiving the prime-boost dosing, 76.2%), the majority mounted strong responses (Fig. 3a) that were comparable with memory responses against CMV, EBV and influenza virus in the same participants (Fig. 3b, c). Individuals immunized with a single dose of 60 μg had a lower response rate (4/9; 44%) and a weaker $CD8^+$ T cell response to RBD. The strength of RBD-specific $CD8^+$ T cell responses correlated positively with vaccine-induced $CD4^+$ T cell responses but did not significantly correlate with SARS-CoV-2 neutralizing antibody titres (Extended Data Fig. 4c, d).

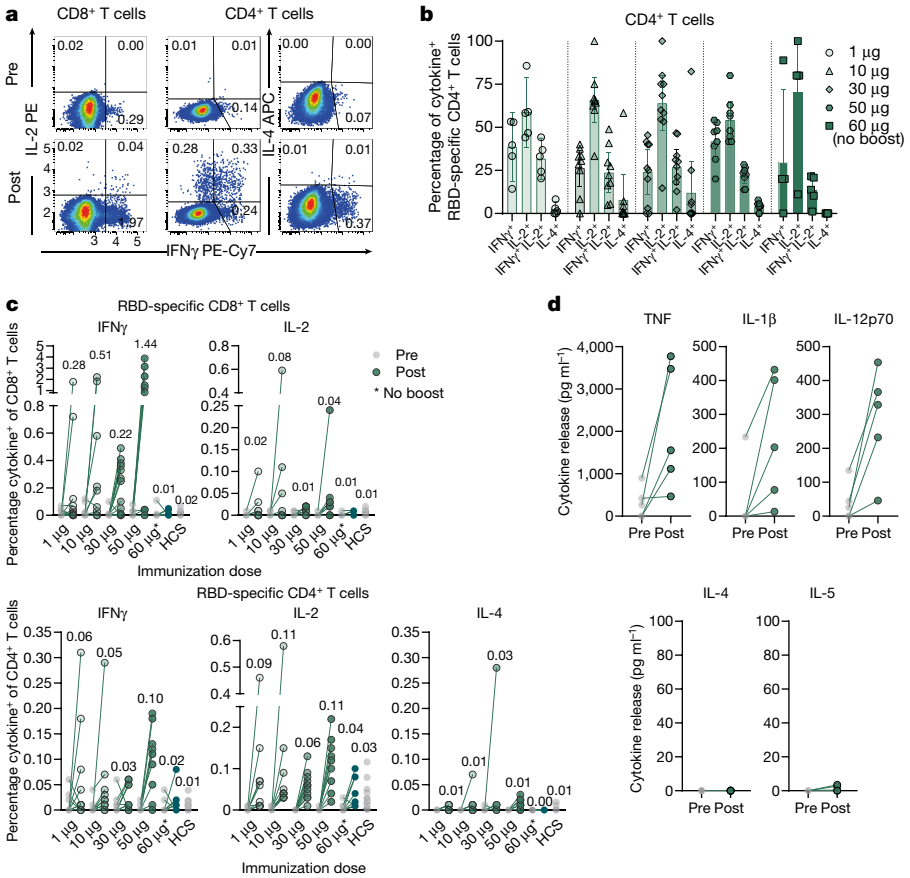

Fig. 4 | Cytokine polarization of BNT162b1-induced T cells. The vaccination schedule is described in Extended Data Fig. 1. PBMCs from vaccinated participants (7 days after boost for cohorts 1 and 10 μg, $n = 10$ each; 30 μg, $n = 12$; 50 μg, $n = 9$; 28 days after prime for the 60 μg cohort, $n = 11$) and donors who had recovered from COVID-19 (HCS, $n = 15$; **c**) were stimulated over night with an overlapping peptide pool representing the vaccine-encoded RBD and analysed by flow cytometry (**a**–**c**) and bead-based immunoassay (**d**). The gating strategy is depicted in Supplementary Fig. 1. **a**, Exemplary pseudocolour flow cytometry plots of cytokine-producing CD4+ and CD8+ T cells from a participant who was immunized with the 10-μg dose. **b**, RBD-specific CD4+ T cells producing the indicated cytokine as a percentage of total cytokine-producing RBD-specific CD4+ T cells. Arithmetic mean with 95% CI. CD4 non-responders (<0.03% total cytokine-producing T cells; 1 μg, $n = 5$; 10 μg, $n = 1$; 30 μg, $n = 2$; 50 μg, $n = 1$; 60 μg, $n = 6$) were excluded. **c**, RBD-specific CD8+ (top) or CD4+ (bottom) T cells producing the indicated cytokine as a percentage of total circulating T cells of the same subset. Values above data points indicate mean fractions per dose cohort. Participants' PBMCs were tested as single instance (**b**, **c**). **d**, Cytokine release by PBMCs from the 50 μg cohort ($n = 5$; assay results from remaining samples of this and other cohorts not available at the time). Each data point represents the mean from duplicate wells subtracted by the DMSO control for one study participant. LLOQs were 6.3 pg ml^{-1} for TNF, 2.5 pg ml^{-1} for IL-1β, 7.6 pg ml^{-1} for IL-12p70, 11.4 pg ml^{-1} for IL-4 and 5.3 pg ml^{-1} for IL-5.

Of note, although at 1 μg BNT162b1 the rates of CD4+ and CD8+ T cell response were lower than for the other doses (9 and 8 out of 11 participants, respectively), the number of vaccine-induced T cells in some participants was almost as high as with 50 μg BNT162b1 (Fig. 3a).

To assess the functionality and polarization of RBD-specific T cells, we identified cytokines secreted in response to stimulation with overlapping peptides representing the full-length sequence of the vaccine-encoded RBD by intracellular staining (ICS) for IFNγ, IL-2 and IL-4 in PBMCs collected before and after vaccination from 52 participants who had been immunized with BNT162b1. RBD-specific CD4+ T cells secreted IFNγ, IL-2, or both, but in most individuals they did not secrete IL-4 (Fig. 4 a–c, Extended Data Table 6). Similarly, fractions of RBD-specific CD8+ T cells secreted IFNγ+ and IL-2.

The mean fraction of RBD-specific T cells within total circulating T cells obtained by BNT162b1 vaccination was substantially higher than that observed in fifteen donors who had recovered from COVID-19. Fractions of RBD-specific IFNγ+ CD8+ T cells reached up to several per cent of total peripheral blood CD8+ T cells in immunized individuals (Fig. 4c). The supernatants of PBMCs from five vaccinated participants were stimulated ex vivo with overlapping RBD peptides and produced the proinflammatory cytokines TNF, IL-1β and IL-12p70, but neither IL-4 nor IL-5 (Fig. 4d).

In summary, these findings indicate that BNT162b1 induces functional and proinflammatory CD4+ and CD8+ T cell responses in almost all participants, with T_H1 polarization of the helper response.

Discussion

We observed concurrent production of neutralizing antibodies, activation of virus-specific CD4+ and CD8+ T cells, and robust release of immune-modulatory cytokines such as IFNγ, which represents a coordinated immune response to counter a viral intrusion[24]. IFNγ is a key cytokine for several antiviral responses. It acts in synergy with type I interferons to inhibit the replication of SARS-CoV[25]. Individuals with polymorphisms in the *IFNG* gene that impair IFNγ activity have a fivefold increase in susceptibility to SARS[26]. The robust elicitation of IFNγ-producing CD8+ T cells indicates that a favourable cellular immune response with anti-viral and immune-augmenting properties complements the strong neutralizing antibody response.

The detection of IFNγ, IL-2 and IL-12p70, but not IL-4 or IL-5, indicates a favourable T_H1 profile and the absence of a potentially deleterious T_H2 immune response. CD4+ and CD8+ T cells may confer long-lasting immune memory against coronaviruses, as indicated in SARS-CoV-1 survivors, in whom CD8+ T cells persisted for 6–11 years[24,27].

Some cases of asymptomatic virus exposure have been associated with cellular immune response without seroconversion, indicating that SARS-CoV-2-specific T cells could be relevant in disease control even in the absence of neutralizing antibodies[28]. In our study, almost all vaccinated volunteers mounted RBD-specific T cell responses that were detected using an ex vivo ELISpot assay, which was performed without prior expansion of T cells and captures only high-magnitude T cell responses. While the strength of the T cell responses varied considerably between participants, we observed no clear dose dependency of the T cell response strength within the tested dose range (1–50 µg). Even with a dose as low as 1 µg, mRNA-encoded immunogen stimulation and robust expansion of T cells was accomplished in most subjects.

Our results confirm the dose-dependency of RBD-binding IgG and neutralization responses and reproduces our previous findings for the 10 and 30 µg dose levels of BNT162b1 in the USA trial[1]. The observed strong boost response for BNT162b1 is in line with the absence of a limiting anti-vector immunity, which is a characteristic advantage of the RNA-based vaccine platform.

The ratio of serum virus neutralization GMT to recombinant RBD-binding IgG GMC is lower after immunization with BNT162b1 than after infection with SARS-CoV-2. As noted previously, this difference may be attributed, in part, to BNT162b1 eliciting antibodies that bind epitopes that are exposed on the RNA-encoded RBD immunogen but buried and inaccessible in the spikes of SARS-CoV-2 virions, differentially increasing RBD-binding IgG GMCs after immunization. In addition, infection with SARS-CoV-2 might elicit neutralizing antibodies that recognize epitopes that are exposed on virions and located outside the RBD, differentially increasing the serum neutralizing GMT after infection[29,30].

As reported for other types of vaccine, mRNA vaccine-induced B cell responses typically peak two weeks after the boost and thereafter drop over time until they reach a sustained memory phase with only gradual decline[31]. The RBD-binding antibody concentrations and SARS-COV-2 neutralizing titres elicited by two doses of BNT162b1 appear to follow this pattern, showing a decline on day 43. A long-term trend based on the contraction phase cannot be extrapolated. A description of the durability of the antibody response to BNT162b1 will emerge over the planned six months of serological follow up in this study and two years of follow up in the corresponding USA study. A distinguishing observation for this RNA-based vaccine candidate is that two injections of BNT162b1 at a dose level as low as 1 µg can induce levels of RBD-binding IgG higher than those observed in convalescent sera, and serum neutralizing antibody titres that were still increasing up to day 43.

As was also observed in the USA trial of this vaccine candidate[1], reactogenicity to BNT162b1 is dose-dependent, and a higher proportion of participants had severe reactogenicity after the second dose, leading to a decision not to admininster a boost at the 60-µg dose level. The number of subjects who reported severe adverse events was more pronounced in the German trial than in the placebo-controlled USA trial. BNT162b1 demonstrated in principle a manageable tolerability at dose levels that elicited robust immune responses. Meanwhile, BNT162b2, which is derived from the same nucleoside-modified vaccine platform but encodes the full spike protein, has been assessed in two clinical trials and has been found to have a milder reactogenicity profile[32]. Based on the more favourable systemic tolerability, BNT162b2 was selected to advance into a phase II/III trial.

Purely RBD-directed immunity might be considered prone to escape of the virus by single amino-acid changes in this small domain. To address this concern, we conducted neutralization assays with 17 pseudotyped viruses, 16 of which enter cells using a spike with a different RBD variant found in circulating strains and one of which uses the dominant spike variant D614G. All 17 variants were efficiently neutralized by the five tested BNT162b1 immune sera. At present, there is probably insufficient immunity to SARS-CoV-2 in the human population to drive antigenic drift. If escape from RBD-elicited immunity were to emerge in the future, the versatility of the RNA platform could facilitate fast adaptation to newly emerging viral strains.

Limitations of our clinical study include the small sample size and its restriction to participants below 55 years of age. Another constraint is that we did not perform further T cell analysis (for example, deconvolution of epitope diversity, characterization of HLA restriction, T cell phenotyping and TCR repertoire analysis) before and after vaccination, because of the limited blood volumes that were available for biomarker analyses. Similarly, we did not assess the induction of tissue-resident memory $CD8^+$ T cells. Further, as vaccine-induced immunity can wane over time, it is important to study the persistence of potentially protective immune responses. Samples to assess persistence are not yet available but are planned in the study protocol and will be reported elsewhere. The results reported here were obtained from immunization with one of four vaccine candidates in the study. Upcoming reports of Project Lightspeed will present the data obtained for other COVID-19 vaccine candidates, including BNT162b2, the RNA-based vaccine candidate that encodes the full-length SARS-CoV-2 spike glycoprotein and is being tested in a phase III efficacy trial[32].

Online content

Any methods, additional references, Nature Research reporting summaries, source data, extended data, supplementary information, acknowledgements, peer review information; details of author contributions and competing interests; and statements of data and code availability are available at https://doi.org/10.1038/s41586-020-2814-7.

1. Mulligan, M. J. et al. Phase 1/2 study of COVID-19 RNA vaccine BNT162b1 in adults. *Nature* https://doi.org/10.1038/s41586-020-2639-4 (2020).
2. WHO. *Coronavirus Disease (COVID-19) Dashboard* (accessed 17 September 2020); https://covid19.who.int/
3. Habibzadeh, P. & Stoneman, E. K. The novel coronavirus: a bird's eye view. *Int. J. Occup. Environ. Med.* **11**, 65–71 (2020).
4. Pardi, N. et al. Nucleoside-modified mRNA vaccines induce potent T follicular helper and germinal center B cell responses. *J. Exp. Med.* **215**, 1571–1588 (2018).
5. Sahin, U., Karikó, K. & Türeci, Ö. mRNA-based therapeutics—developing a new class of drugs. *Nat. Rev. Drug Discov.* **13**, 759–780 (2014).
6. Pardi, N. et al. Zika virus protection by a single low-dose nucleoside-modified mRNA vaccination. *Nature* **543**, 248–251 (2017).
7. Pardi, N. et al. Characterization of HIV-1 nucleoside-modified mRNA vaccines in rabbits and rhesus macaques. *Mol. Ther. Nucleic Acids* **15**, 36–47 (2019).
8. Sahin, U. et al. An RNA vaccine drives immunity in checkpoint-inhibitor-treated melanoma. *Nature* **585**, 107–112 (2020).
9. Rauch, S., Jasny, E., Schmidt, K. E. & Petsch, B. New vaccine technologies to combat outbreak situations. *Front. Immunol.* **9**, 1963 (2018).
10. Pardi, N. et al. Expression kinetics of nucleoside-modified mRNA delivered in lipid nanoparticles to mice by various routes. *J. Control. Release* **217**, 345–351 (2015).
11. Pardi, N. et al. Nucleoside-modified mRNA immunization elicits influenza virus hemagglutinin stalk-specific antibodies. *Nat. Commun.* **9**, 3361 (2018).
12. Tai, W. et al. A recombinant receptor-binding domain of MERS-CoV in trimeric form protects human dipeptidyl peptidase 4 (hDPP4) transgenic mice from MERS-CoV infection. *Virology* **499**, 375–382 (2016).
13. Holtkamp, S. et al. Modification of antigen-encoding RNA increases stability, translational efficacy, and T-cell stimulatory capacity of dendritic cells. *Blood* **108**, 4009–4017 (2006).
14. Orlandini von Niessen, A. G. et al. Improving mRNA-based therapeutic gene delivery by expression-augmenting 3′ UTRs identified by cellular library screening. *Mol. Ther.* **27**, 824–836 (2019).
15. Karikó, K. et al. Incorporation of pseudouridine into mRNA yields superior nonimmunogenic vector with increased translational capacity and biological stability. *Mol. Ther.* **16**, 1833–1840 (2008).
16. Tsai, M. Y. et al. Effect of influenza vaccine on markers of inflammation and lipid profile. *J. Lab. Clin. Med.* **145**, 323–327 (2005).
17. Taylor, D. N. et al. Development of VAX128, a recombinant hemagglutinin (HA) influenza-flagellin fusion vaccine with improved safety and immune response. *Vaccine* **30**, 5761–5769 (2012).
18. Doener, F. et al. RNA-based adjuvant CV8102 enhances the immunogenicity of a licensed rabies vaccine in a first-in-human trial. *Vaccine* **37**, 1819–1826 (2019).
19. Destexhe, E. et al. Evaluation of C-reactive protein as an inflammatory biomarker in rabbits for vaccine nonclinical safety studies. *J. Pharmacol. Toxicol. Methods* **68**, 367–373 (2013).
20. Kamphuis, E., Junt, T., Waibler, Z., Forster, R. & Kalinke, U. Type I interferons directly regulate lymphocyte recirculation and cause transient blood lymphopenia. *Blood* **108**, 3253–3261 (2006).
21. Baum, A. et al. Antibody cocktail to SARS-CoV-2 spike protein prevents rapid mutational escape seen with individual antibodies. *Science* **369**, 1014–1018 (2020).
22. Zhang, L. et al. The D614G mutation in the SARS-CoV-2 spike protein reduces S1 shedding and increases infectivity. Preprint at https://www.biorxiv.org/content/10.1101/2020.06.12.148726v1 (2020).

23. Sette, A. et al. Selective CD4+ T cell help for antibody responses to a large viral pathogen: deterministic linkage of specificities. *Immunity* **28**, 847–858 (2008).
24. Vabret, N. et al. Immunology of COVID-19: current state of the science. *Immunity* **52**, 910–941 (2020).
25. Sainz, B., Jr, Mossel, E. C., Peters, C. J. & Garry, R. F. Interferon-beta and interferon-gamma synergistically inhibit the replication of severe acute respiratory syndrome-associated coronavirus (SARS-CoV). *Virology* **329**, 11–17 (2004).
26. Chong, W. P. et al. The interferon gamma gene polymorphism +874 A/T is associated with severe acute respiratory syndrome. *BMC Infect. Dis.* **6**, 82 (2006).
27. Ng, O.-W. et al. Memory T cell responses targeting the SARS coronavirus persist up to 11 years post-infection. *Vaccine* **34**, 2008–2014 (2016).
28. Gallais, F. *et al*. Intrafamilial exposure to SARS-CoV-2 induces cellular immune response without seroconversion. Preprint at https://www.medrxiv.org/content/10.1101/2020.06.21.20132449v1 (2020).
29. Chi, X. et al. A neutralizing human antibody binds to the N-terminal domain of the Spike protein of SARS-CoV-2. *Science* **369**, 650–655 (2020).
30. Brouwer, P. J. M. et al. Potent neutralizing antibodies from COVID-19 patients define multiple targets of vulnerability. *Science* **369**, 643–650 (2020).
31. Feldman, R. A. et al. mRNA vaccines against H10N8 and H7N9 influenza viruses of pandemic potential are immunogenic and well tolerated in healthy adults in phase 1 randomized clinical trials. *Vaccine* **37**, 3326–3334 (2019).
32. Walsh, E. E. et al. RNA-Based COVID-19 vaccine BNT162b2 selected for a pivotal efficacy study. Preprint at https://www.medrxiv.org/content/10.1101/2020.08.17.20176651v2 (2020).

Publisher's note Springer Nature remains neutral with regard to jurisdictional claims in published maps and institutional affiliations.

© The Author(s), under exclusive licence to Springer Nature Limited 2020

Methods

Clinical trial design

Study BNT162-01 (NCT04380701) is an ongoing, first-in-human, phase I/II, open-label dose-ranging clinical trial to assess the safety, tolerability, and immunogenicity of ascending dose levels of various intramuscularly administered BNT162 mRNA vaccine candidates in healthy men and non-pregnant women 18 to 55 years of age (amended to add 56–85 years of age). Key exclusion criteria included previous clinical or microbiological diagnosis of COVID-19; receipt of medications to prevent COVID-19; previous vaccination with any coronavirus vaccine; a positive serological test for SARS-CoV-2 IgM and/or IgG; and a SARS-CoV-2 NAAT-positive nasal swab; those with increased risk for severe COVID-19; and immunocompromised individuals. The primary endpoints of the study are safety and immunogenicity.

In the part of the study reported here, five dose levels (1 µg, 10 µg, 30 µg, 50 µg or 60 µg) of the BNT162b1 candidate were assessed at one site in Germany with 12 healthy participants per dose level in a dose-escalation/de-escalation design. Sentinel dosing was performed in each dose-escalation cohort. Progression in that cohort and dose escalation required data review by a safety review committee. Participants received a BNT162b1 prime dose on day 1, and a boost dose on day 22 ± 2. Serum for antibody assays was obtained on days 1 (pre-prime), 8 ± 1 (post-prime), 22 ± 2 (pre-boost), 29 ± 3 and 43 ± 4 (post-boost). PBMCs for T cell studies were obtained on days 1 (pre-prime) and 29 ± 3 (post-boost). Tolerability was assessed by patient diary. One individual in the 10 µg cohort and one in the 50 µg cohort left the study before the boosting immunization owing to withdrawal of consent for private reasons.

The presented data comprise the BNT162b1-immunized cohorts only and are based on a preliminary analysis with a data extraction date of 23 July 2020, focused on analysis of vaccine-induced immunogenicity (secondary endpoint) descriptively summarized at the various time points and on reactogenicity. All participants for whom data were available were included in the immunogenicity analyses.

The trial was carried out in Germany in accordance with the Declaration of Helsinki and Good Clinical Practice Guidelines and with approval by an independent ethics committee (Ethik-Kommission of the Landesärztekammer Baden-Württemberg, Stuttgart, Germany) and the competent regulatory authority (Paul-Ehrlich Institute, Langen, Germany). All participants provided written informed consent.

Manufacturing of RNA

BNT162b1 incorporates a Good Manufacturing Practice (GMP)-grade mRNA drug substance that encodes the trimerized SARS-CoV-2 spike glycoprotein RBD antigen. The RNA is generated from a DNA template by in vitro transcription in the presence of 1-methylpseudouridine-5′-triphosphate (m1ΨTP; Thermo Fisher Scientific) instead of uridine-5′-triphosphate (UTP). Capping is performed co-transcriptionally using a trinucleotide cap 1 analogue ($(m_2^{7,3'\text{-}O})$Gppp($m^{2'\text{-}O}$)ApG; TriLink). The antigen-encoding RNA contains sequence elements that increase RNA stability and translation efficiency in human dendritic cells[13,14]. The mRNA is formulated with lipids to obtain the RNA–LNP drug product. The vaccine was transported and supplied as a buffered-liquid solution for intramuscular injection and was stored at −80 °C.

Proteins and peptides

A pool of 15-mer peptides that overlapped by 11 amino acids and covered the whole sequence of the BNT162b1-encoded SARS-CoV-2 RBD was used for ex vivo stimulation of PBMCs for flow cytometry, IFNγ ELISpot and cytokine profiling. CEF (CMV, EBV, influenza virus; human leukocyte antigen (HLA) class I epitope peptide pool) and CEFT (CMV, EBV, influenza virus, tetanus toxoid; HLA class II epitope peptide pool) (both JPT Peptide Technologies) were used as controls for general T cell reactivity.

Human convalescent sera and PBMC panel

Human SARS-CoV-2 infection/COVID-19 convalescent sera (n = 38) were drawn from donors 18–83 years of age at least 14 days after PCR-confirmed diagnosis and at a time when the participants were asymptomatic. The mean age of the donors was 45 years. Neutralizing GMTs in subgroups of the donors were as follows: symptomatic infections, 90 (n = 35); asymptomatic infections, 156 (n = 3); hospitalized, 618 (n = 1). Sera were obtained from Sanguine Biosciences (Sherman Oaks, CA), the MT Group (Van Nuys, CA) and Pfizer Occupational Health and Wellness (Pearl River, NY). Human SARS-CoV-2 infection/COVID-19 convalescent PBMC samples (n = 15) were collected from donors 22–79 years of age 30–62 days after PCR-confirmed diagnosis when donors were asymptomatic. PBMC donors had asymptomatic or mild infections (n = 13; clinical score 1 and 2) or had been hospitalized (n = 2; clinical score 4 and 5). Blood samples were obtained from the Frankfurt University Hospital (Germany).

Cell culture and primary cell isolation

Vero cells (CCL-81) and Vero E6 cells (ATCC CRL-1586) were sourced from the American Type Culture Collection (ATCC), which maintains a quality management system commensurate to ISO 9001:2015, ISO 13485:2016, ISO 17025:2017, and ISO 17034:2016. Cells were certified by the vendor and cultured in Dulbecco's modified Eagle's medium (DMEM) with GlutaMAX (Gibco) supplemented with 10% fetal bovine serum (FBS) (Sigma-Aldrich). Cell lines were tested for mycoplasma contamination after receipt and before expansion and cryopreservation. PBMCs were isolated by Ficoll-Hypaque (Amersham Biosciences) density gradient centrifugation and cryopreserved before subsequent analysis.

RBD-binding IgG assay

A recombinant SARS-CoV-2 RBD containing a C-terminal Avitag (Acro Biosystems) was bound to streptavidin-coated Luminex microspheres. Heat-inactivated participant sera were diluted to 1:500, 1:5,000, and 1:50,000. Following overnight incubation at 2–8 °C while shaking, plates were washed in a solution containing 0.05% Tween-20. A secondary R-PE-labelled goat anti-human IgG polyclonal antibody (1:500; Jackson Labs) was added for 90 min at room temperature while shaking, before plates were washed once more in a solution containing 0.05% Tween-20. Data were captured as median fluorescent intensities (MFIs) using a Bioplex200 system (Bio-Rad) and converted to U/ml antibody concentrations using a reference standard curve (reference standard composed of a pool of five convalescent serum samples obtained more than 14 days after COVID-19 PCR diagnosis and diluted sequentially in antibody-depleted human serum) with arbitrarily assigned concentrations of 100 U/ml and accounting for the serum dilution factor. Three dilutions were used to increase the likelihood that at least one result for any sample would fall within the useable range of the standard curve. Assay results are reported in U/ml of IgG. The final assay results were expressed as the GMC of all sample dilutions that produced a valid assay result within the assay range.

SARS-CoV-2 neutralization assay

The neutralization assay used a previously described strain of SARS-CoV-2 (USA_WA1/2020) that had been rescued by reverse genetics and engineered by the insertion of an mNeonGreen (mNG) gene into open reading frame 7 of the viral genome[33]. This reporter virus generates similar plaque morphologies and indistinguishable growth curves from wild-type virus. Viral master stocks (2×10^7 PFU/ml) were grown in Vero E6 cells as previously described[33]. With patient convalescent sera, the fluorescent neutralization assay produced comparable results to the conventional plaque reduction neutralization assay[34]. Serial dilutions of heat-inactivated sera were incubated with the reporter virus (2×10^4 PFU per well to yield a 10–30% infection rate of the Vero CCL81 monolayer) for 1 h at 37 °C before inoculating Vero CCL81 cell

monolayers (targeted to have 8,000 to 15,000 cells in a central field of each well at the time of seeding, 24 h before infection) in 96-well plates to allow accurate quantification of infected cells. Total cell counts per well were enumerated by nuclear stain (Hoechst 33342) and fluorescent virally infected foci were detected 16–24 h after inoculation with a Cytation 7 Cell Imaging Multi-Mode Reader (BioTek) with Gen5 Image Prime version 3.09. Titres were calculated in GraphPad Prism version 8.4.2 by generating a four-parameter (4PL) logistical fit of the percentage neutralization at each serial serum dilution. The 50% neutralization titre (VNT_{50}) was reported as the interpolated reciprocal of the dilution yielding a 50% reduction in fluorescent viral foci.

VSV-SARS-CoV-2 spike variant pseudovirus neutralization assay

Vesicular stomatitis virus (VSV)-SARS-CoV-2-S pseudoparticle generation and neutralization assays were performed as previously described[21]. In brief, human codon-optimized SARS-CoV-2 spike (GenBank: MN908947.3) was synthesized (Genscript) and cloned into an expression plasmid. SARS-CoV-2 complete genome sequences were downloaded from GISAID nucleotide database (https://www.gisaid.org) on 20 March 2020, as described previously[21]. Sequences were curated and the genetic diversity of the spike-encoding gene was assessed across high-quality genome sequences using custom pipelines. Amino acid substitutions were cloned into the spike expression plasmid using site-directed mutagenesis. HEK293T cells (ATCC CRL-3216) were seeded (culture medium: DMEM high glucose (Life Technologies) supplemented with 10% heat-inactivated FBS (Life Technologies), 90.1 units/ml penicillin, 90.1 µg/ml streptomycin and 0.26 mg/ml L-glutamine (Life Technologies)) and transfected the following day with spike expression plasmid using Lipofectamine LTX (Life Technologies) following the manufacturer's protocol. At 24 h post-transfection at 37 °C, cells were infected with the VSVΔG:mNeon/VSV-G diluted in Opti-MEM (Life Technologies) at a multiplicity of infection of 1. Cells were incubated for 1 h at 37 °C, washed to remove residual input virus and overlaid with infection medium (DMEM high glucose supplemented with 0.7% low IgG BSA (Sigma), 1 mM sodium pyruvate (Life Technologies) and 0.05 µg/ml gentamicin (Life Technologies)). After 24 h at 37 °C, the supernatant containing VSV-SARS-CoV-2-S pseudoparticles was collected, centrifuged at 3,000*g* for 5 min to clarify and stored at −80 °C until further use.

For pseudovirus neutralization assays, Vero cells (ATCC CCL-81) were seeded in 96-well plates in culture medium and allowed to reach approximately 85% confluence before use in the assay (24 h later). Sera were serially diluted 1:2 in infection medium starting with a 1:40 dilution. VSV-SARS-CoV-2-S pseudoparticles were diluted 1:1 in infection medium for a fluorescent focus unit (ffu) count in the assay of ~1,000. Serum dilutions were mixed 1:1 with pseudoparticles for 30 min at room temperature before addition to Vero cells and incubation at 37 °C for 24 h. Supernatants were removed and replaced with PBS (Gibco), and fluorescent foci were quantified using the SpectraMax i3 plate reader with MiniMax imaging cytometer (Molecular Devices). Neutralization titres were calculated in GraphPad Prism version 8.4.2 by generating a 4PL fit of the percentage neutralization at each serial serum dilution. The $pVNT_{50}$ was reported as the interpolated reciprocal of the dilution yielding a 50% reduction in fluorescent viral foci.

IFNγ ELISpot

IFNγ ELISpot analysis was performed ex vivo (without further in vitro culturing for expansion) using PBMCs depleted of $CD4^+$ and enriched for $CD8^+$ T cells ($CD8^+$ effectors), or depleted of $CD8^+$ and enriched for $CD4^+$ T cells ($CD4^+$ effectors). Tests were performed in duplicate and with a positive control (anti-CD3 monoclonal antibody (1:1,000; Mabtech)). Multiscreen filter plates (Merck Millipore) pre-coated with IFNγ-specific antibodies (ELISpotPro kit, Mabtech) were washed with PBS and blocked with X-VIVO 15 medium (Lonza) containing 2% human serum albumin (CSL-Behring) for 1–5 h. Per well, 3.3×10^5 effector cells were stimulated for 16–20 h with an overlapping peptide pool representing the vaccine-encoded RBD. Bound IFNγ was visualized using a secondary anti-IFNγ antibody directly conjugated with alkaline phosphatase (1:250; ELISpotPro kit, Mabtech) followed by incubation with a 5-bromo-4-chloro-3′-indolyl phosphate (BCIP)/nitro blue tetrazolium (NBT) substrate (ELISpotPro kit, Mabtech). Plates were scanned using an AID Classic Robot ELISPOT Reader and analysed by AID ELISPOT 7.0 software (AID Autoimmun Diagnostika). Spot counts were summarized as mean values of each duplicate. T cell responses stimulated by peptides were compared to effectors incubated with medium only as a negative control using an in-house ELISpot data analysis tool (EDA), based on two statistical tests (distribution-free resampling) as described[35,36], to provide sensitivity while maintaining control over false positives.

To account for varying sample quality reflected in the number of spots in response to anti-CD3 antibody stimulation, a normalization method was applied to enable direct comparison of spot counts/strength of response between individuals. This dependency was modelled in a log-linear fashion with a Bayesian model including a noise component (unpublished). For a robust normalization, each normalization was sampled 10,000 times from the model and the median taken as normalized spot count value. Likelihood of the model $\log\lambda_E = \alpha\log\lambda_P + \log\beta_j + \sigma\varepsilon$, where λ_E is the normalized spot count of the sample, α is a stable factor (normally distributed) common among all positive controls λ_P, β_j is a sample *j*-specific component (normally distributed) and $\sigma\varepsilon$ is the noise component, of which σ is Cauchy distributed and ε is Student's *t*-distributed. β_j ensures that each sample is treated as a different batch.

Flow cytometry

Cytokine-producing T cells were identified by intracellular cytokine staining. PBMCs thawed and rested for 4 h in OpTmizer medium supplemented with 2 µg/ml DNase I (Roche) were restimulated with a peptide pool representing the vaccine-encoded SARS-CoV-2 RBD (2 µg/ml/peptide; JPT Peptide Technologies) in the presence of GolgiPlug (BD) for 18 h at 37 °C. Controls were treated with DMSO-containing medium. Cells were stained for viability and surface markers (CD3 BV421, 1:250; CD4 BV480, 1:50; CD8 BB515, 1:100; all BD Biosciences) in flow buffer (DPBS (Gibco) supplemented with 2% FBS (Biochrom), 2 mM EDTA (EDTA; Sigma-Aldrich) for 20 min at 4 °C. Afterwards, samples were fixed and permeabilized using the Cytofix/Cytoperm kit according to the manufacturer's instructions (BD Biosciences). Intracellular staining was performed in Perm/Wash buffer for 30 min at 4 °C (CD3 BV421, 1:250; CD4 BV480, 1:50; CD8 BB515, 1:100; IFNγ PE-Cy7, 1:50; IL-2 PE, 1:10; IL-4 APC, 1:500; all BD Biosciences). Samples were acquired on a fluorescence-activated cell sorter (FACS) VERSE instrument (BD Biosciences) using BD FACSuite software version 1.0.6 and analysed with FlowJo software version 10.5.3 (FlowJo LLC, BD Biosciences). RBD-specific cytokine production was corrected for background by subtraction of values obtained with dimethyl sulfoxide (DMSO)-containing medium. Negative values were set to zero. Cytokine production in Fig. 4b was calculated by summing the fractions of all $CD4^+$ T cells positive for IFNγ, IL-2 or IL-4, setting this sum to 100% and calculating the fraction of each specific cytokine-producing subset thereof. Pseudocolour plot axes are in $\log_{10}$ scale.

Cytokine profiling

Human PBMCs were restimulated for 48 h with SARS-CoV-2 RBD peptide pool (2 µg/ml final concentration per peptide). Stimulation with DMSO-containing medium served as negative controls. Concentrations of tumour necrosis factor (TNF), IL-1β, IL-12p70, IL-4 and IL-5 in supernatants were determined using a bead-based, 11-plex T_H1/T_H2 human ProcartaPlex immunoassay (Thermo Fisher Scientific) according to the manufacturer's instructions. Fluorescence was measured with a Bio-plex200 system (Bio-Rad) and analysed with ProcartaPlex Analyst 1.0 software (Thermo Fisher Scientific). RBD-specific cytokine production

was corrected for background by subtraction of values obtained with DMSO-containing medium. Negative values were set to zero.

Statistical analysis

The sample size for the reported part of the study was not based on statistical hypothesis testing. All participants with data available were included in the safety and immunogenicity analyses. The statistical method of aggregation used for the analysis of antibody concentrations and titres is the geometric mean and the corresponding 95% CI. Using the geometric mean allows us to account for non-normal distribution of antibody concentrations and titres spanning several orders of magnitude. Spearman correlation was used to evaluate the monotonic relationship between non-normally distributed data sets. All statistical analyses were performed using GraphPad Prism software version 8.4.2. The experiments were not randomized and the investigators were not blinded to allocation during experiments and outcome assessment.

Reporting summary

Further information on research design is available in the Nature Research Reporting Summary linked to this paper.

Data availability

The data that support the findings of this study are available from the corresponding author upon reasonable request. SARS-CoV-2 complete genome sequences were downloaded from the GISAID nucleotide database (https://www.gisaid.org) on 20 March 2020, as described previously[21]. Upon completion of this clinical trial, summary-level results will be made public and shared in line with data sharing guidelines.

33. Xie, X. et al. An Infectious cDNA Clone of SARS-CoV-2. *Cell Host Microbe* **27**, 841–848.e3 (2020).
34. Muruato, A. E. et al. A high-throughput neutralizing antibody assay for COVID-19 diagnosis and vaccine evaluation. *Nat. Commun.* **11**, 4059 (2020).
35. Moodie, Z., Huang, Y., Gu, L., Hural, J. & Self, S. G. Statistical positivity criteria for the analysis of ELISpot assay data in HIV-1 vaccine trials. *J. Immunol. Methods* **315**, 121–132 (2006).
36. Moodie, Z. et al. Response definition criteria for ELISPOT assays revisited. *Cancer Immunol. Immunother.* **59**, 1489–1501 (2010).
37. U.S. Department of Health and Human Services. Toxicity grading scale for healthy adult and adolescent volunteers enrolled in preventive vaccine clinical trials. https://www.fda.gov/regulatory-information/search-fda-guidance-documents/ toxicity-grading-scale-healthy-adult-and-adolescent-volunteers-enrolled-preventive-vaccine-clinical (2007).

Acknowledgements We thank M. Dolsten for advice during drafting of the manuscript; C. Anders, C. Anft, N. Beckmann, K. Bissinger, G. Boros, P. Cienskowski, K. Clarke, C. Ecker, A. Engelmann, Y. Feuchter, L. Heesen, M. Hossainzadeh, S. Jägle, L. Jeck, O. Kahl, M. Knezovic, T. Kotur, M. Kretschmer, O. Pfante, J. Reinholz, L.-M. Schmid, R. Schulz, B. Stock, C. Müller, S. Murphy, G. Szabó and M. Vehreschild for technical support, project management and advice; A. Finlayson and M. Rao for editorial assistance; P. Koch and F. Groher for data management and analysis; S. Liebscher and O. Kistner for expert advice; J. Absalon for manuscript advice; the CRS Team (Mannheim and Berlin) for study conduct: S. Baumann, M. Berse, M. Casjens, B. Ehrlich, and F. Seitz; the Pfizer Vaccines Clinical Assays Team and the Pfizer Aviation Team for technical and logistical support of serology analyses; and the GISAID Nucleotide database for sharing of SARS-CoV-2 complete genome sequences. BioNTech is the sponsor of the study and responsible for the design, data collection, data analysis, data interpretation and writing of the report. Pfizer advised on the study and the manuscript, generated serological data and contracted for the generation of serological data. The corresponding authors had full access to all the data in the study and had final responsibility for the decision to submit the data for publication. All study data were available to all authors. This study was not supported by any external funding at the time of submission.

Author contributions U.S. conceived and conceptualized the work and strategy, supported by Ö.T. Experiments were planned or supervised by E.D., C.F.-G., C.A.K., L.M.K., U.L., A.M., J.Q., P.-Y.S. and I.V. A.B., D.C., M.C., C.F.-G., W.K., K.P., J.Q., I.L.S. and P.-Y.S. performed experiments. D.B., S. Brachtendorf, E.D., P.R.D., J.G., K.U.J., A.-K.E., L.M.K., M.-C.K., V.L., A.M., J.Q., J.S., I.V. and M.V. analysed data. D.M. planned and supervised dashboards for analysis of clinical trial data. R.H. was responsible for data normalization and adaption. C.B. and C.R. were responsible for biomarker and R&D program management. K.K. optimized the mRNA. M.B., S. Bolte, B.F., A.K.-B., D.L., T.P. and A.S. coordinated operational conduct of the clinical trial. J.L.P. advised on the trial, and J.L. and K.A.S. advised on experiments. U.S. and Ö.T., supported by M.B., E.D., P.R.D., K.U.J., L.M.K., A.M., I.V. and M.V., interpreted data and wrote the manuscript. All authors supported the review of the manuscript.

Competing interests All authors have completed the International Committee of Medical Journal Editors (ICMJE) uniform disclosure form at https://www.gisaid.orgwww.icmje.org/coi_disclosure.pdf˙ and declare: U.S. and Ö.T. are management board members and employees at BioNTech SE (Mainz, Germany); D.B., C.B., S. Brachtendorf, E.D., A.-K.E., B.F., J.G., R.H., M.-C.K., U.L., V.L., D.M., C.R., J.S. and T.P. are employees at BioNTech SE; K.K., L.M.K., I.V., A.M., J.Q. and M.V. are employees at BioNTech RNA Pharmaceuticals GmbH; M.B. is an employee at Bexon Clinical Consulting LLC. A.B., C.A.K. and K.P. are employees of Regeneron Pharmaceuticals Inc; K.K., A.M., U.S. and Ö.T. are inventors on patents and patent applications related to RNA technology and COVID-19 vaccine; D.B., C.B., S. Bolte, E.D., J.G., K.K., R.H., A.K.-B., L.M.K., D.L., U.L., A.M., C.R., U.S., Ö.T., I.V. and M.V. have securities from BioNTech SE; D.C., M.C., P.R.D., K.U.J., W.K., J.L., J.L.P., I.L.S. and K.A.S. are employees at Pfizer and may have securities from Pfizer; C.A.K. is an officer at Regeneron Pharmaceuticals, Inc; A.B., C.A.K. and K.P. have securities from Regeneron Pharmaceuticals, Inc; C.F.-G. and P.-Y.S. received compensation from Pfizer to perform the neutralization assay; no other relationships or activities that could appear to have influenced the submitted work.

Additional information

Supplementary information is available for this paper at https://doi.org/10.1038/s41586-020-2814-7.

Correspondence and requests for materials should be addressed to U.S.

Peer review information *Nature* thanks Barbra Richardson and the other, anonymous, reviewer(s) for their contribution to the peer review of this work.

Reprints and permissions information is available at http://www.nature.com/reprints.

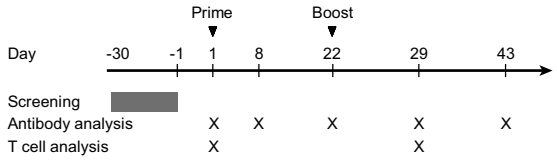

Extended Data Fig. 1 | Schedule of vaccination and assessment. Study participants received a prime immunisation with BNT162b1 on day 1 (all dose levels), and a boost immunisation on day 22 ± 2 (all dose levels except 60 μg). Serum was obtained on day 1 (pre-prime), 8 ± 1 (post-prime), 22 ± 2 (pre-boost), 29 ± 3 and 43 ± 4 (post-boost). PBMCs were obtained on day 1 (pre-prime) and 29 ± 3 (post-boost).

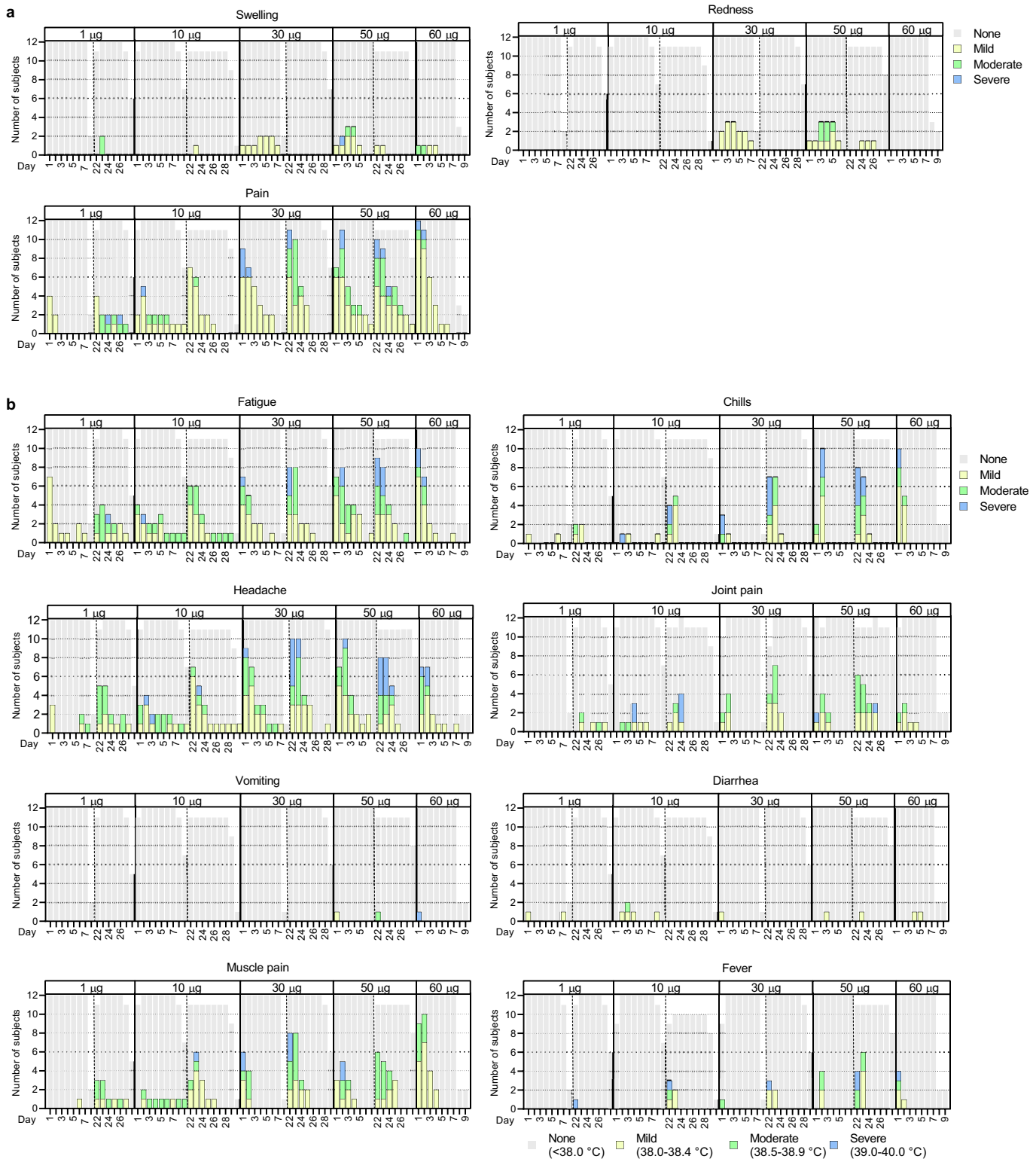

Extended Data Fig. 2 | Solicited adverse events. Number of participants with local (**a**) or systemic solicited adverse events (AEs) (**b**). Participants were immunised with BNT162b1 on days 1 (all dose levels) and 22 (all dose levels except 60 µg). $n = 12$ subjects were injected per group, from day 22 on $n = 11$ for the 10 µg and 50 µg cohort due to discontinuation of patients due to non-vaccine related reasons. Grey shading indicates number of participants at each time point. As per protocol, AEs were recorded up to 7 days after each immunisation (days 1-7 and 22-28) to determine reactogenicity; for some participants 1-2 additional days of follow-up were available. Grading of AEs was performed according to US Food and Drug Administration (FDA) recommendations[37].

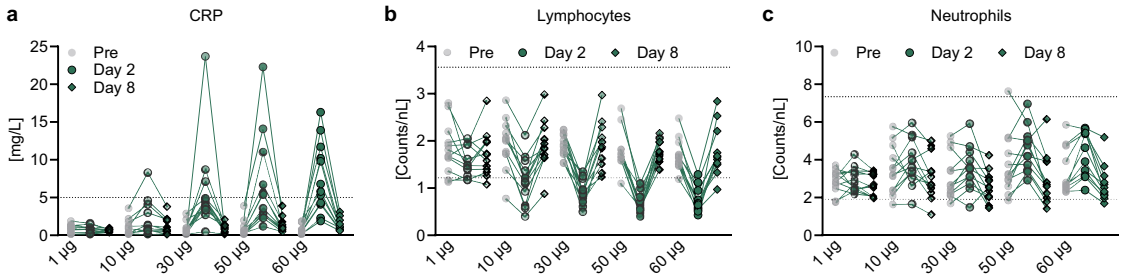

Extended Data Fig. 3 | Pharmacodynamic markers. Participants were immunised with BNT162b1 on days 1 (all dose levels) and 22 (all dose levels except 60 µg) ($n = 12$ per group, from day 22 on $n = 11$ for the 10 µg and 50 µg cohort). **a**, Kinetics of C-reactive protein (CRP) level. **b**, Kinetics of lymphocyte counts. **c**, Kinetics of neutrophil counts. Dotted lines indicate upper and lower limit of reference range. For values below the lower limit of quantification (LLOQ) = 0.3, LLOQ/2 values were plotted (**a**).

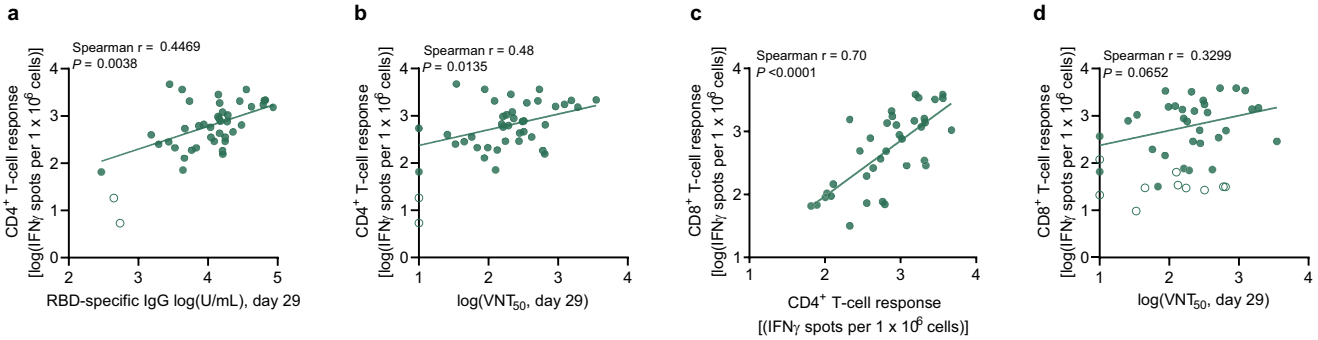

Extended Data Fig. 4 | Correlation of antibody and T cell responses. Participants were immunised with BNT162b1 on days 1 (all dose levels) and 22 (all dose levels except 60 µg) ($n = 12$ per group, from day 22 on $n = 11$ for the 10 µg and 50 µg cohort). Data are plotted for all prime/boost vaccinated participants (cohorts 1, 10, 30 and 50 µg) with data points for participants with no detectable T cell response (open circles; **a**, **b**, **d**) excluded from correlation analysis. Nonparametric Spearman correlation. **a**, Correlation of RBD-specific IgG responses (as in Fig. 1) with $CD4^+$ T cell responses on day 29 (as in Fig. 3). r = 0.4829, $P = 0.0014$. **b**, Correlation of VNT_{50} (as in Fig. 2a) with $CD4^+$ T cell responses (as in Fig. 3). r = 0.48, $P = 0.0057$. **c**, Correlation of $CD4^+$ with $CD8^+$ T cell responses ($n = 51$ as in Fig. 3a) from day 29 in dose cohorts 1 to 60 µg. r = 0.7, $P < 0.0001$. **d**, Correlation of VNT_{50} (as in Fig. 2a) with $CD8^+$ T cell responses (as in Fig. 3) on day 29. r = 0.3299, $P = 0.0652$.

Extended Data Table 1 | Demographic characteristics

Cohort		1 µg (N=12) n (%)	10 µg (N=12) n (%)	30 µg (N=12) n (%)	50 µg (N=12) n (%)	60 µg (N=12) n (%)	Total (N=60) n (%)
Sex	Male	5 (41.7)	4 (33.3)	8 (66.7)	6 (50.0)	7 (58.3)	30 (50.0)
	Female	7 (58.3)	8 (66.7)	4 (33.3)	6 (50.0)	5 (41.7)	30 (50.0)
Race	Caucasian	12 (100)	11 (91.7)	12 (100)	12 (100)	11 (91.7)	58 (96.7)
	African American	0	1 (8.3)	0	0	0	1 (1.7)
	Asian	0	0	0	0	1 (8.3)	1 (1.7)
Age at vaccination (years)	Mean (SD)	38.21 (10.48)	43.62 (11.03)	35.74 (8.60)	33.88 (10.72)	35.81 (12.50)	37.5 (10.91)
	Median	39.8	46.6	35.2	30.8	30.1	36.0
	Min, Max	21.4, 55.8	25.1, 55.0	23.9, 54.0	19.9, 47.8	20.9, 53.2	19.9, 55.8

N, number of subjects in the specified group. This value is the denominator for the percentage calculations. n, number of subjects with the specified characteristics.

Extended Data Table 2 | Subject disposition and analysis sets

	BNT162b1 vaccinated		Antibody analysis					T-cell analysis	
Cohort	Prime	Boost	Day 1	Day 8±1	Day 22±2	Day 29±3	Day 43±4	Day 1	Day 29±3
1 µg	12	12	12	12	12	12	12	10* (10)	11 (10)
10 µg	12	11	12	12	12	11	11	11 (10)	11 (10)
30 µg	12	12	12	12	12	12	12	10 (12)	10 (12)
50 µg	12	11	12	12	12	11	11	10 (9)	10 (9)
60 µg	12	N/A	12	12	11	12	12	9 (11)	9 (11)

Antibody analysis: Values indicate number of participants for whom virus neutralisation assays and RBD binding IgG antibody assays were performed. T cell analysis: Values indicate number of participants for whom IFNγ ELISpot and flow cytometry (values in parentheses) were performed. N/A, not applicable. *9 for $CD4^+$ response data.

Extended Data Table 3 | BNT162b1-induced geometric mean RBD-binding IgG concentrations and 95% confidence intervals

Dose	-	1 µg				10 µg				30 µg				50 µg				60 µg				HCS
Day	Pre	8	22	29	43	8	22	29	43	8	22	29	43	8	22	29	43	8	22	29	43	-
N	60	12	12	12	12	12	12	11	11	12	12	12	12	12	12	11	11	12	11	12	12	38
Geometric mean	1.6	2.6	265	2,015	3,920	1.1	826	9,107	6,707	1.9	1,273	17,051	12,431	1.3	1,672	25,006	18,289	1.2	909	1,058	755	602
Lower 95% CI	1.1	1.3	104	948	1,915	0.58	295	5,290	3,383	0.89	655	10,534	7,900	0.61	992	14,228	10,029	0.57	438	590	521	350
Upper 95% CI	2.1	5.2	676	4,284	8,023	2.3	2,316	15,676	13,296	3.9	2,475	27,600	19,559	2.9	2,818	43,950	33,350	2.5	1,887	1,899	1,094	1,034

Geometric mean RBD-binding IgG concentration values and 95% confidence intervals by cohort and sampling time-point as displayed in Fig. 1. CI, confidence interval; N, Sample number; HCS, Human COVID-19 convalescent sample.

Extended Data Table 4 | BNT162b1-induced virus geometric mean 50% neutralization titers and 95% confidence intervals

Dose	-	1 µg				10 µg				30 µg				50 µg				60 µg				HCS
Day	Pre	8	22	29	43	8	22	29	43	8	22	29	43	8	22	29	43	8	22	29	43	-
N	60	12	12	12	12	12	12	11	11	12	12	12	12	12	12	11	11	12	11	12	12	38
Geometric mean	10	10	12	36	62	10	21	11	11	10	28	308	157	10	32	578	333	10	19	20	17	94
Lower 95% CI	10	10	8.9	18	31	10	12	90	57	10	15	165	86	10	19	331	176	10	12	13	12	62
Upper 95% CI	10	10	17	71	123	10	36	278	276	10	51	574	288	10	54	1,009	631	10	28	30	25	142

Geometric mean 50% virus neutralisation titer values (VNT_{50}) and 95% confidence intervals by cohort and sampling time-point as displayed in Fig. 2a. CI, confidence interval; N, Sample number; HCS, Human COVID-19 convalescent sample.

Extended Data Table 5 | BNT162b1-induced geometric mean 50% pseudovirus neutralization titers and 95% confidence intervals

Variant	WT	Q321L	V341I	A348T	N354D	S359N	V367F	K378R	R408I	Q409E	A435S	K458R	I472V	G476S	V483A	Y508H	H519P	D614G
N	5	5	5	5	5	5	5	5	5	5	5	5	5	5	5	5	5	5
GMT	2,948	1,898	1,561	3,302	3,411	4,563	7,668	3,280	5,879	2,872	3,776	3,711	2,055	3,641	3,824	1,916	5,352	3,822
Lower 95% CI	1,413	867	767	1,417	1,556	1,737	3,441	1,414	2,601	1,115	1,552	1,850	907	1,547	1,368	896	1,784	1,460
Upper 95% CI	6,151	4,155	3,175	7,692	7,479	11,982	17,088	7,611	13,285	7,400	9,187	7,444	4,655	8,570	10,695	4,093	16,059	10,010

Geometric mean 50% pseudovirus neutralisation titer ($pVNT_{50}$) values and 95% confidence intervals by tested SARS-CoV-2 spike protein variants as displayed in Fig. 2c. CI, confidence interval; N, Sample number; HCS, Human COVID-19 convalescent sample; Variant, SARS-CoV-2 spike protein variant.

Extended Data Table 6 | BNT162b1-induced mean cytokine values and 95% confidence intervals

Dose	1 μg				10 μg				30 μg				50 μg				60 μg			
Cytokines	IFNγ$^+$	IL-2$^+$	IFNγ$^+$ IL-2$^+$	IL-4$^+$	IFNγ$^+$	IL-2$^+$	IFNγ$^+$ IL-2$^+$	IL-4$^+$	IFNγ$^+$	IL-2$^+$	IFNγ$^+$ IL-2$^+$	IL-4$^+$	IFNγ$^+$	IL-2$^+$	IFNγ$^+$ IL-2$^+$	IL-4$^+$	IFNγ$^+$	IL-2$^+$	IFNγ$^+$ IL-2$^+$	IL-4$^+$
N	5	5	5	5	9	9	9	9	10	10	10	10	8	8	8	8	5	5	5	5
Mean	39	59	32	2.5	26	66	24	7.9	24	64	27	12	42	54	22	4.0	30	70	14	0.0
Lower 95% CI	19	38	20	0	16	53	12	0	11	48	17	0	32	43	17	1.7	0	28	3.1	0.0
Upper 95% CI	59	79	44	6.8	37	79	35	23	37	80	37	30	51	65	26	6.3	72	113	24	0.0

Mean values and 95% confidence intervals for the individual cytokines tested as in Fig. 4b. CI, confidence interval; N, Sample number.

nature research

Corresponding author(s): Ugur Sahin

Last updated by author(s): Sep 16, 2020

Reporting Summary

Nature Research wishes to improve the reproducibility of the work that we publish. This form provides structure for consistency and transparency in reporting. For further information on Nature Research policies, see Authors & Referees and the Editorial Policy Checklist.

Statistics

For all statistical analyses, confirm that the following items are present in the figure legend, table legend, main text, or Methods section.

n/a	Confirmed	
☐	☒	The exact sample size (*n*) for each experimental group/condition, given as a discrete number and unit of measurement
☐	☒	A statement on whether measurements were taken from distinct samples or whether the same sample was measured repeatedly
☒	☐	The statistical test(s) used AND whether they are one- or two-sided *Only common tests should be described solely by name; describe more complex techniques in the Methods section.*
☒	☐	A description of all covariates tested
☒	☐	A description of any assumptions or corrections, such as tests of normality and adjustment for multiple comparisons
☐	☒	A full description of the statistical parameters including central tendency (e.g. means) or other basic estimates (e.g. regression coefficient) AND variation (e.g. standard deviation) or associated estimates of uncertainty (e.g. confidence intervals)
☐	☒	For null hypothesis testing, the test statistic (e.g. *F*, *t*, *r*) with confidence intervals, effect sizes, degrees of freedom and *P* value noted *Give P values as exact values whenever suitable.*
☐	☒	For Bayesian analysis, information on the choice of priors and Markov chain Monte Carlo settings
☒	☐	For hierarchical and complex designs, identification of the appropriate level for tests and full reporting of outcomes
☐	☒	Estimates of effect sizes (e.g. Cohen's *d*, Pearson's *r*), indicating how they were calculated

Our web collection on statistics for biologists contains articles on many of the points above.

Software and code

Policy information about availability of computer code

Data collection

Flow cytometry data was collected using the FACS VERSE instrument (BD Biosciences) and FACSSuite software version 1.0.6 and analysed with FlowJo software version 10.5.3 (FlowJo LLC, BD Biosciences).
ELISpot plates were scanned using an AID Classic Robot ELISPOT Reader and analysed by AID ELISPOT 7.0 software (AID Autoimmun Diagnostika).
RBD binding IgG data were captured as median fluorescent intensities (MFIs) using a Luminex reader.
For SARS-CoV-2 neutralisation assay, total cell counts per well were enumerated by nuclear stain (Hoechst 33342) and fluorescent virally infected foci were detected with a Cytation 7 Cell Imaging Multi-Mode Reader (Biotek) with Gen5 Image Prime version 3.09.
For VSV-SARS-CoV-2 spike variant pseudovirus neutralisation assay, fluorescent foci were quantified using the SpectraMax i3 plate reader with MiniMax imaging cytometer (Molecular Devices).
Cytokine profiles in PBMC supernatants were determined using a bead-based, 11-plex TH1/TH2 human ProcartaPlex immunoassay (Thermo Fisher Scientific) according to the manufacturer's instructions and fluorescence was measured with a Bioplex200 system (Bio-Rad).
No custom software codes have been developed.

Data analysis

Flow cytometry data was analysed using FlowJo software version 10.5.3 (FlowJo LLC, BD Biosciences).
ELISpot assays were analysed using AID ELISPOT 7.0 software (AID Autoimmun Diagnostika). T-cell responses stimulated by peptides were compared to T-cell responses stimluated with cell culture medium only as a negative control using an in-house ELISpot data analysis tool (EDA), based on two statistical tests (distribution-free resampling) according to Moodie et al. (refer to Material&Methods section in the manuscript for references), to provide sensitivity while maintaining control over false positives.
RBD binding IgG data captured as median fluorescent intensities (MFIs) were converted to U/mL antibody concentrations using a reference standard curve (reference standard composed of a pool of five convalescent serum samples obtained >14 days post-COVID-19 PCR diagnosis and diluted sequentially in antibody-depleted human serum) with arbitrarily assigned concentrations of 100 U/mL and accounting for the serum dilution factor.
For SARS-CoV-2 and VSV-SARS-CoV-2 spike variant pseudovirus neutralisation assay, titers were calculated in GraphPad Prism version 8.4.2 by generating a 4-parameter (4PL) logistical fit of the percent neutralisation at each serial serum dilution. The 50% neutralisation

titre (VNT50) was reported as the interpolated reciprocal of the dilution yielding a 50% reduction in fluorescent viral foci.
Cytokine profiles in PBMC supernatants were analysed using ProcartaPlex Analyst 1.0 software (Thermo Fisher Scientific).
All statistical analyses were performed using GraphPad Prism software version 8.4.2.

For manuscripts utilizing custom algorithms or software that are central to the research but not yet described in published literature, software must be made available to editors/reviewers. We strongly encourage code deposition in a community repository (e.g. GitHub). See the Nature Research guidelines for submitting code & software for further information.

Data

Policy information about availability of data

All manuscripts must include a data availability statement. This statement should provide the following information, where applicable:

- Accession codes, unique identifiers, or web links for publicly available datasets
- A list of figures that have associated raw data
- A description of any restrictions on data availability

The data that support the findings of this study are available from the corresponding author upon reasonable request. SARS-CoV-2 complete genome sequences were downloaded from GISAID nucleotide database (https://www.gisaid.org) on March 20th, 2020 as referred in Baum et al., 2020. Upon completion of this clinical trial, summary-level results will be made public and shared in line with data sharing guidelines.

Field-specific reporting

Please select the one below that is the best fit for your research. If you are not sure, read the appropriate sections before making your selection.

☒ Life sciences ☐ Behavioural & social sciences ☐ Ecological, evolutionary & environmental sciences

For a reference copy of the document with all sections, see nature.com/documents/nr-reporting-summary-flat.pdf

Life sciences study design

All studies must disclose on these points even when the disclosure is negative.

Sample size	In the part of the clinical study reported here five dose levels (1 µg, 10 µg, 30 µg, 50 µg or 60 µg) of the BNT162b1 vaccine candidate were assessed at one site in Germany with 12 healthy volunteers per dose level in a dose escalation and de-escalation design. Sentinel dosing was performed in each dose-escalation cohort. The inclusion of 12 subjects per group is considered to be adequate for a safety assessment of each vaccine per dose level. The probability to observe a particular TEAE with incidence of 15% at least once in 12 subjects per group is 85.8%.
Data exclusions	Clinical data available until data extraction date of 13JUL2020 were included. All participants with data available were included in the safety and immunogenicity analyses. For serology/cell-mediated immunity correlation analyses (Ext. Data Fig. 4 a/b/d), data were only plotted for prime/boost vaccinated participants (excluding the 60 µg dose level cohort) with detectable T-cell response. All participants with sufficient PBMC material available were included in the ICS analyses. In Fig. 4b, CD4 non-responders (<0.03% total cytokine producing T cells; 1 µg, n=5; 10 µg, n=1; 30 µg, n=2; 50 µg, n=1; 60 µg, n=6) were excluded. All participants with sufficient PBMC material available were included in the ELISPOT analyses. In Fig.3c, participants without a T-cell response were excluded, and data from the 60 µg cohort were excluded. In Ext. Data Fig. 4c, only data from participants with both CD4+ and CD8+ T-cell responses were included. For cytokine analysis in Fig. 4d, only assay results from n=5 participants of the 50 µg cohort were available by the time of submission/re-submission. The remaining samples from this and other cohorts were prioritized for other analyses. Data shown are preliminary and not fully source-data verified.
Replication	A parallel clinical study of very similar design has been conducted in the USA involving the same populations, vaccine candidates and doses. The results for safety and immunogenicity align closely. The US study is randomized placebo controlled. Serology: Participant sera were tested in duplicate and geometric mean concentration (RBD-specific IgG dLIA) or titer (virus neutralisation and pseudovirus neutralisation assay) were plotted. T cell immunity: Participant PBMCs were tested as single instance in ICS analyses. Participant PBMCs were tested in duplicates in ELISpot analyses. Spot counts were summarized as mean values of each duplicate. Data shown are preliminary and not fully source-data verified.
Randomization	Randomization was not performed in order to facilitate operational efficiencies with the sentinel design, also knowing that a parallel randomized, placebo-controlled study was being conducted in the same vaccine constructs in the USA.
Blinding	This is a non-randomized open-label phase I/II trial. Investigators were not blinded in order to facilitate operational efficiencies with the sentinel design, also knowing that a parallel randomized, placebo-controlled study was being conducted in the same vaccine constructs in the USA.

Reporting for specific materials, systems and methods

We require information from authors about some types of materials, experimental systems and methods used in many studies. Here, indicate whether each material, system or method listed is relevant to your study. If you are not sure if a list item applies to your research, read the appropriate section before selecting a response.

Materials & experimental systems

n/a	Involved in the study
☐	☒ Antibodies
☐	☒ Eukaryotic cell lines
☒	☐ Palaeontology
☒	☐ Animals and other organisms
☐	☒ Human research participants
☐	☒ Clinical data

Methods

n/a	Involved in the study
☒	☐ ChIP-seq
☐	☒ Flow cytometry
☒	☐ MRI-based neuroimaging

Antibodies

Antibodies used

Flow cytometry (specificity/host+reactivity/fluorochrome/clone/manufacturer/catalogue number/lot number/dilution/extra- or intracellular):
CD3/mouse anti-human/BV421/UCHT1/BD Biosciences/562426/9113553/1:250/extracellular+intracellular
CD4/mouse anti-human/BV480/RPA-T4/BD Biosciences/746541/0171955/1:50/extracellular+intracellular
CD8/mouse anti-human/BB515/RPA-T8/BD Biosciences/564526/0037189/1:100/extracellular+intracellular
IFNγ /mouse anti-human/PE-Cy7/B27/BD Biosciences/557643/9332967/1:50/intracellular
IL-2/rat anti-human/PE/MQ1-17H12/BD Biosciences/554566/9337013/1:10/intracellular
IL-4/rat anti-human/APC/MP4-25D2/BD Biosciences/554486/9185677/1:500/intracellular

Fixable Viability Dye/eF780/eBioscience/65-0865-14/2185428/1:1,666

ELISpotPro kit/cat. no. 3420-2APT-10/lot no. 370/Mabtech:
Primary anti-IFNg antibody/clone c1-D1K/pre-coated plates
Secondary anti-IFNg antibody/clone 7-B6-1 (ALP conjugate)/1:250
CD3/clone CD3-2/1:1,000

RBD-binding IgG assay:
goat anti-human IgG/R-PE/polyclonal/Jackson Labs/109-115-098/147186/1:500

Validation

Commercially available antibodies were selected based on their antigen specificity and suggested application as described on the manufacturer`s website and data sheets. The antibody concentrations for staining were optimized by titrating down each reagent starting at the manufacturer`s recommendation. The optimal amounts of the reagents were defined by (i) minimal unspecific shift of the negative population and (ii) a maximal separation of the negative and positive population. Individual antibody validation reports are not evident from the BD Biosciences website.

Eukaryotic cell lines

Policy information about cell lines

Cell line source(s)

Vero cells (CCL-81), Vero E6 cells (CRL-1586) and HEK293T (CRL-3216) were obtained from ATCC.

Authentication

Vero and Vero E6 cells were sourced from ATCC, which maintains a quality management system commensurate to ISO 9001:2015, ISO 13485:2016, ISO 17025:2017, and ISO 17034:2016. Cells were certified by the vendor and propagated according to the manufacturer's instructions.

Mycoplasma contamination

All used cell lines were tested negative for mycoplasma contamination after receipt and before expansion and cryopreservation.

Commonly misidentified lines
(See ICLAC register)

No commonly misidentified cell lines were used.

Human research participants

Policy information about studies involving human research participants

Population characteristics

Healthy men and non-pregnant women 18 to 55 years (amended to add 56 -85 of age) of age with equal gender distribution. Most participants were Caucasian (96.7%) with one African American and one Asian subject (1.7% each). Key exclusion criteria included previous clinical or microbiological diagnosis of COVID-19; receipt of medications to prevent COVID-19; previous vaccination with any coronavirus vaccine; a positive serological test for SARS-CoV-2 IgM and/or IgG at the screening visit; and a SARS-CoV-2 NAAT-positive nasal swab within 24 hours before study vaccination; those with increased risk for severe COVID-19; immunocompromised individuals, those with known infection with HIV, hepatitis C virus, or hepatitis B virus and those with a history of autoimmune disease.

Recruitment

Recruitment was performed by teaching investigators according to inclusion and exclusion criteria without any bias. No protocol-specified methods. The sites are experienced phase 1 units with established rostas of potential subjects who they can invite for screening for inclusion. Also the sites advertise through their own web-site. Some subjects self-referred via the sponsor.

Ethics oversight	The trial was carried out in Germany in accordance with the Declaration of Helsinki and Good Clinical Practice Guidelines and with approval by an independent ethics committee (Ethik-Kommission of the Landesärztekammer Baden-Württemberg, Stuttgart, Germany) and the competent regulatory authority (Paul-Ehrlich Institute, Langen, Germany). All subjects provided written informed consent.

Note that full information on the approval of the study protocol must also be provided in the manuscript.

Clinical data

Policy information about clinical studies

All manuscripts should comply with the ICMJE guidelines for publication of clinical research and a completed CONSORT checklist must be included with all submissions.

Clinical trial registration	ClinicalTrials.gov Identifier: NCT04380701, see also manuscript
Study protocol	The full clinical study protocol is not published online, but a comprehensive description of the clinical trial design, eligibility criteria and endpoints is available at https://clinicaltrials.gov/ct2/show/study/NCT04380701.
Data collection	Serum for antibody assays was obtained on day 1 (pre-prime), 8±1 (post-prime), 22±2 (pre-boost), 29±3 and 43±4 (post-boost). PBMCs for T cell studies were obtained on day 1 (pre-prime) and 29±3 (post-boost). Tolerability was assessed by patient diary. All formal protocol-determined visits were conducted on-site at the investigators premises (in each case a dedicated phase 1 unit). All study procedures such as blood sample, physical examinations, screening checks were conducted at the study sites. The only exceptions were the completion of the subject diaries, which was done by the subjects at home. Diaries were collected by the sites at the subjects' next scheduled visits and the data entered on site. There was also dedicated telephone follow-up, 48 hrs following dosing, to ensure subject well-being, which was documented on site by the investigator conducting the call.
Outcomes	Primary objective: To describe the safety and tolerability profiles of prophylactic BNT162 vaccines in healthy adults after single dose (SD; prime only) or prime/boost (P/B) immunization. Endpoints: Solicited local reactions & solicited systemic reactions (listed in subject diaries, to be graded by subjects) and unsolicited treatment-emergent adverse events. Secondary objectives: To describe the immune response in healthy adults after SD or P/B immunization measured by a functional antibody titer, e.g., virus neutralization test or an equivalent assay available by the time of trial conduct. Endpoints: Functional antibody responses; fold increasese in functional antibody titers; number of subjects with seroconversion

Flow Cytometry

Plots

Confirm that:

☒ The axis labels state the marker and fluorochrome used (e.g. CD4-FITC).

☒ The axis scales are clearly visible. Include numbers along axes only for bottom left plot of group (a 'group' is an analysis of identical markers).

☒ All plots are contour plots with outliers or pseudocolor plots.

☒ A numerical value for number of cells or percentage (with statistics) is provided.

Methodology

Sample preparation	Cytokine-producing T cells were identified by intracellular cytokine staining. PBMCs thawed and rested for 4 hours in OpTmizer medium supplemented with 2 µg/mL DNAseI (Roche), were restimulated with a peptide pool representing the vaccine-encoded SARS-CoV-2 RBD (2 µg/mL/peptide; JPT Peptide Technologies) in the presence of GolgiPlug (BD) for 18 hours at 37 °C. Controls were treated with DMSO-containing medium. Cells were stained for viability and surface markers in flow buffer ((DPBS (Gibco) supplemented with 2% FCS (Biochrom), 2 mM EDTA (Sigma-Aldrich)) for 20 minutes at 4 °C. Afterwards, samples were fixed and permeabilized using the Cytofix/Cytoperm kit according to manufacturer's instructions (BD Biosciences). Intracellular staining was performed in Perm/Wash buffer for 30 minutes at 4 °C.
Instrument	Samples were acquired on a FACS VERSE instrument (BD Biosciences).
Software	For data analysis FlowJo software version 10.5.3 (FlowJo LLC, BD Biosciences) was used.
Cell population abundance	Bulk PBMCs were used. No cell sorting was performed.
Gating strategy	The gating strategies are detailed in the respective figure or in the supplementary information. Briefly, singlets were gated based on their location in the FSC-A/FSC-H plot. Debris was exclduded in the subsequent FSC-A/viability dye plot. Viable cells were gated from non-debris in the FSC-A/viability dye plot. From viable cells, lymphocytes were gated based on their size and granularity in the FSC-A/SSC-A plot. From lymphocytes, CD3+ T cells were gated in the CD3/SSC-A plot. From CD3+ T cells, CD4+ and CD8+ T cells were gated in the CD4/CD8 plot. From CD4+ T cells, IFNg+, IL-2+, IL-4+ or IFNg+ IL-2+ T cells were gated by plotting CD4/IFNg, CD4/IL-2, CD4/IL-4, or IFNg/IL-2. From CD8+ T cells, IFNg+, IL-2+ or IFNg+ IL-2+ T cells were gated by plotting CD8/IFNg, CD8/IL-2, or IFNg/IL-2.

☒ Tick this box to confirm that a figure exemplifying the gating strategy is provided in the Supplementary Information.